1915

The role of myelin geometry on magnetic susceptibility-driven frequency shifts: toward realistic geometries

Tianyou Xu[1], Sean Foxley[1], Michiel Kleinnijenhuis[1], and Karla Miller[1]

[1]*Oxford Centre for Functional Magnetic Resonance Imaging of the Brain, University of Oxford, Oxford, Oxfordshire, United Kingdom*

Background: Recent work from several groups has described the magnetic susceptibility anisotropy χ_a of myelin as a significant contributor to MR phase contrast.[1-5] Incorporation of χ_a resolves some of the inconsistencies observed between biophysical models and experimental results on frequency shifts; however, incongruities still remain, such as which source(s) precisely is/are responsible for the size and orientation dependence of the myelin water frequency.[4] A diversity of microstructural geometries exist in white matter. Previous works have modeled axons as nested cylinders.[4-6] In reality, axons vary in eccentricity and in deformity. While simulations consisting categorically of circles benefit from simplicity the consequences of this simplifying assumption have not been studied. If the ultimate goal of this research is to noninvasively extract microstructure parameters such as g-ratio (which quantifies the extent of myelination) and/or axon density, a careful and thorough understanding of the role of shape in the modulation of the MR signal is essential.

Purpose: This abstract investigates the role that the geometry of myelin has on susceptibility driven frequency shifts in white matter. Our work builds on previous studies which have examined field distributions on the scales of single and packed axons.[5,6] Packed axons, representative of axon bundles, capture important aspects of tissue microstructure.[6] Here we demonstrate via simulation that axonal shape has a nontrivial effect on the underlying distribution of proton frequencies and on the free induction decay signal magnitude and phase. To bridge simulation with physical reality, we derive a structural template from electron microscopy (EM) in excised white matter, which is then used to forward calculate the frequency distribution and signal.

Basic Model: Magnetic field perturbations are simulated using the susceptibility tensor formulation in the Fourier framework, allowing for the accommodation of susceptibility anisotropy.[7] χ_a is described by a rank 2 tensor whose diagonal elements represent the longitudinal and perpendicular tensor components of the radial myelin unit.[1,3,5] A value of -10 E-6 was selected for both χ_a and $\chi_{isotropic}$, which is within the range of estimated values.[3,5] A three-compartment axon model was used to generate the complex FID signal, described by the equation below where f_n represents all frequencies in compartment n. Other parameters are listed in the table. Simulations were performed in 2D assuming that the static field (set to 3 Tesla) is orthogonal to the axons. Axons are considered to be infinite in the 3rd dimension. EM data on mouse corpus callosum was acquired at a resolution of 11nm and hand segmented to derive a more realistic representation of microstructural compartment geometry.

$$\chi_{ij} = \chi_{iso}\, I_2 + \chi_a \begin{pmatrix} 1 & 0 & 0 \\ 0 & -\frac{1}{2} & 0 \\ 0 & 0 & -\frac{1}{2} \end{pmatrix}$$

$$S(t) = \sum_{n=1}^{3} \rho_n\, e^{-t/T_{2,n}}\, e^{i\,2\,\pi\,t\,f_n}$$

Parameters	Myelin	Axonal	Extra-Axonal
T2	25 ms	75 ms	75 ms
Proton Density	0.5	1	1
$\Delta\chi_{anisotropic/isotropic}$	-10 E -6	0	0

Model Results: Field perturbations of elliptical axons of increasing eccentricity and varying orientations (in the x-y plane) are shown in Fig A-F (color-map scales from -10 to 15 Hz). Each case generates a distinct magnitude and phase profile with differences in phase being more pronounced (Fig H). Area fractions of myelin, axonal and extra axonal space are conserved across all cases. We extend these simulations to consider a field of packed axons spanning ~60x60 µm with Gamma-distributed radius (mean 0.5 µm), Gaussian-distributed g-ratio (mean 0.67).[8] The axon packing density ~83%. We compare the frequency distribution from circular and elliptically deformed ("warped") axons. Frequency distributions were obtained by sampling a central region within the packing (compared for the three compartments in Fig I). In both simulations the distribution associated with the intra-axonal space is sharply defined ~ -3.8 Hz. This value precisely matches what the input g-ratio (mean 0.67) dictates, a relation that has been derived analytically.[1,5] The effect of non-circularity that is captured in the frequency distribution is further reflected through differences in the observed signal magnitude and phase (Fig J-K), particularly the phase. The results until here demonstrate that deviations of circularity modulate the underlying frequency distribution at both the level of single axons as well as axon bundles. However, these conclusions are driven by idealized geometries. To reproduce physical reality we acquired EM data to provide a structural template from which we forward calculate the field perturbations. This preliminary result uses only a portion of an SEM, 4.1x4.1 µm, which was hand-segmented to identify the myelin sheath. This is compared to an idealized circular packing with matching axon and myelin fractions as well as spatial location, representing the classical interpretation of axonal packing. The non circular nature of axons gives rise to a different frequency distribution and consequently distinct signal magnitude and phase evolutions (Fig L-N).

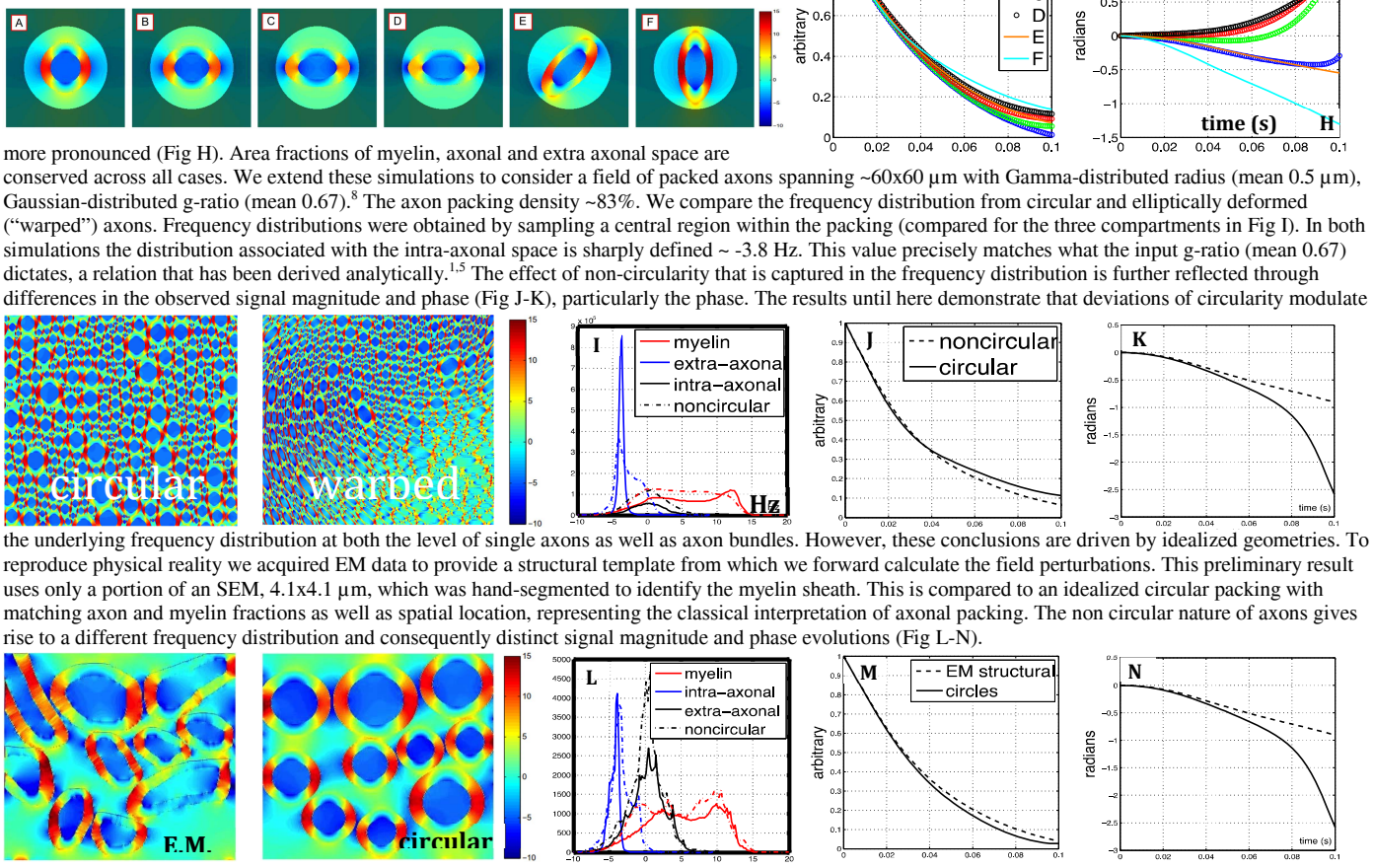

Conclusions: Simulation of white matter in the context of magnetic susceptibility is significantly affected by myelin geometry. Since an ultimate goal in this field is to extract microstructure parameters such as g-ratio and axon density from the MR signal a careful and thorough understanding of the role of shape in the modulation of this signal is essential. **Acknowledgements:** University of Oxford's Clarendon Trust Graduate Scholarship and the Wellcome Trust.

Citations: **(1)** Sukstanskii et al. MRM 2014 **(2)** Wharton et al. MRM 2014 **(3)** Lee et al. PNAS 2010 **(4)** Sati et al. Neuroimage 2013 **(5)** Wharton et al. PNAS 2012 **(6)** Chen et al. Neuroimage 2013 **(7)** Liu C. MRM 2010 **(8)** Barazany et al. Brain 2009.